A momentum-space Argonne V18 interaction

S. Veerasamy and W. N. Polyzou

Department of Physics and Astronomy,

The University of Iowa, Iowa City, IA 52242

(Dated: January 14, 2011)

Abstract

This paper gives two representations of the Argonne V18 potential in momentum space. One is as an expansion in terms elementary functions and other as an expansion in terms of Chebyshev polynomials. Both provide practical and efficient representations for computing the momentum-space potential that does not require integration or interpolation. Programs based on both expansions are available as supplementary material.

PACS numbers: 21.45.Bc ,21.30.Cb

I. INTRODUCTION

The Argonne V18 potential [**?**] is one of a number of realistic nucleon-nucleon interactions [**?**][**?**][**?**]. It is distinguished from other realistic interactions because it is expressed as an operator expansion with local configuration-space coefficient functions. This representation has advantages when used in variational Monte Carlo calculations. On the other hand there are a number of calculations that require a realistic interaction that are more naturally performed in momentum space. These include some Faddeev calculations, relativistic few-body calculations, and electromagnetic calculations. In the momentum representation the variable conjugate to the relative coordinate is the difference between the final and initial momenta. In calculations, both momenta appear, which requires a separate Fourier transform for each pair of momenta. While the direct Fourier transforms of the V18 potential have been used in some applications, this is not the most efficient method to calculate the Fourier transform of the potential. The purpose of this paper is to provide useful, tested, easily reproducible analytic forms of the Fourier transform of the Argonne V18 potential for use in momentum-space calculations. The analytic forms allow for a direct calculation of the momentum-space interaction for any pair of initial and final momenta. In keeping with the traditional Argonne form, the momentum-space potential is given in operator form. The resulting momentum space potential has 24 terms. This is because the $\mathbf{L}^2 V(r)$ and $(\mathbf{L}\cdot\mathbf{S})^2 V(r)$ operators become linear combinations of two momentum-space operators with different coefficient functions. In this work the Fourier transform is applied to the strong part of the Argonne V18 potential, without the electromagnetic terms. The Argonne V18 potential has the form

$$V = \sum_{n=1}^{18} V_n(r) O_n \tag{1.1}$$

where $V_n(r)$ are rotationally invariant coefficient functions of the relative coordinate of the nucleons and the O_n are the following set of eighteen spin-isospin operators:

$$O_1 = I, \qquad O_2 = (\boldsymbol{\tau}_1\cdot\boldsymbol{\tau}_2), \qquad O_3 = (\boldsymbol{\sigma}_1\cdot\boldsymbol{\sigma}_2), \tag{1.2}$$

$$O_4 = (\mathbf{s}_1\cdot\mathbf{s}_2)(\boldsymbol{\tau}_1\cdot\boldsymbol{\tau}_2), \qquad O_5 = S_{12} = 3(\boldsymbol{\sigma}_1\cdot\hat{\mathbf{r}})(\boldsymbol{\sigma}_2\cdot\hat{\mathbf{r}}) - \boldsymbol{\sigma}_1\cdot\boldsymbol{\sigma}_2, \qquad O_6 = S_{12}(\boldsymbol{\tau}_1\cdot\boldsymbol{\tau}_2), \tag{1.3}$$

$$O_7 = (\mathbf{L}\cdot\mathbf{S}), \qquad O_8 = (\mathbf{L}\cdot\mathbf{S})(\boldsymbol{\tau}_1\cdot\boldsymbol{\tau}_2) \qquad O_9 = (\mathbf{L}\cdot\mathbf{L}) \tag{1.4}$$

$$O_{10} = (\mathbf{L}\cdot\mathbf{L})(\boldsymbol{\tau}_1\cdot\boldsymbol{\tau}_2), \qquad O_{11} = (\mathbf{L}\cdot\mathbf{L})(\boldsymbol{\sigma}_1\cdot\boldsymbol{\sigma}_2), \qquad O_{12} = (\mathbf{L}\cdot\mathbf{L})(\boldsymbol{\sigma}_1\cdot\boldsymbol{\sigma}_2)(\boldsymbol{\tau}_1\cdot\boldsymbol{\tau}_2), \tag{1.5}$$

$$O_{13} = (\mathbf{L}\cdot\mathbf{S})^2, \qquad O_{14} = (\mathbf{L}\cdot\mathbf{S})^2(\boldsymbol{\tau}_1\cdot\boldsymbol{\tau}_2), \qquad O_{15} = T_{12} = (3\tau_{1z}\tau_{2z} - \boldsymbol{\tau}\cdot\boldsymbol{\tau}), \tag{1.6}$$

$$O_{16} = (\boldsymbol{\sigma}_1\cdot\boldsymbol{\sigma}_2)T_{12}, \qquad O_{17} = S_{12}T_{12}, \qquad O_{18} = (\tau_{1z}+\tau_{2z}). \tag{1.7}$$

where T_{12} is the isotensor operator $T_{12} := 3\tau_{1z}\tau_{2z} - \boldsymbol{\tau}_1\cdot\boldsymbol{\tau}_2$. While the isospin operators, $\boldsymbol{\tau}_i$, factor out of the Fourier transforms, the operators L^2, $\mathbf{L}\cdot\mathbf{S}$, $(\mathbf{L}\cdot\mathbf{S})^2$ and the tensor operator S_{12} contribute to the Fourier transform.

For the eighteen operators there are four types of integrals that must be computed to calculate the Fourier transforms. The potential matrix element $\langle\mathbf{k}'|V|\mathbf{k}\rangle$, with $\mathbf{q} := \mathbf{k} - \mathbf{k}'$, has the following contributions:

1. Identity

$$\frac{1}{(2\pi)^3}\int e^{-i(\mathbf{k}'-\mathbf{k})\cdot\mathbf{r}}V_j(r)d\mathbf{r} = \frac{1}{2\pi^2}\int_0^\infty j_0(qr)V_j(r)r^2dr \tag{1.8}$$

2. $\mathbf{L}\cdot\mathbf{S}$

$$\frac{1}{(2\pi)^3}\int e^{-i\mathbf{k}'\cdot\mathbf{r}}V_j(r)\mathbf{L}\cdot\mathbf{S}e^{i\mathbf{k}\cdot\mathbf{r}}d\mathbf{r} = i\mathbf{k}\times\mathbf{k}'\frac{1}{2\pi^2 q}\int_0^\infty j_1(qr)V_j(r)r^3dr \tag{1.9}$$

3. $\mathbf{L}\cdot\mathbf{L}$

$$\frac{1}{(2\pi)^3}\int e^{-i\mathbf{k}'\cdot\mathbf{r}}V_j(r)\mathbf{L}\cdot\mathbf{L}e^{i\mathbf{k}\cdot\mathbf{r}}d\mathbf{r} =$$

$$-(\mathbf{k}'\times\mathbf{k})\cdot(\mathbf{k}'\times\mathbf{k})\frac{1}{2\pi^2q^2}\int_0^\infty j_2(qr)V_j(r)r^4dr + 2(\mathbf{k}'\cdot\mathbf{k})\frac{1}{2\pi^2 q}\int_0^\infty j_1(qr)V_j(r)r^3dr \tag{1.10}$$

4 $(\mathbf{L}\cdot\mathbf{S})^2$

$$\frac{1}{(2\pi)^3}\int e^{-i\mathbf{k}'\cdot\mathbf{r}}V_j(r)(\mathbf{L}\cdot\mathbf{S})^2e^{i\mathbf{k}\cdot\mathbf{r}}d\mathbf{r} =$$

$$-(\mathbf{S}\cdot(\mathbf{k}\times\mathbf{k}'))^2\frac{1}{2\pi^2q^2}\int_0^\infty j_2(qr)V_j(r)r^4dr + (\mathbf{k}'\times\mathbf{S})\cdot(\mathbf{k}\times\mathbf{S})\frac{1}{2\pi^2 q}\int_0^\infty j_1(qr)V_j(r)r^3dr \tag{1.11}$$

5. $S_{12} = 3(\hat{\mathbf{r}}\cdot\boldsymbol{\sigma}_1)(\hat{\mathbf{r}}\cdot\boldsymbol{\sigma}_2) - \boldsymbol{\sigma}_1\cdot\boldsymbol{\sigma}_2$

$$\frac{1}{(2\pi)^3}\int e^{-i\mathbf{k}'\cdot\mathbf{r}}V(r)\left(3(\hat{\mathbf{r}}\cdot\boldsymbol{\sigma}_1)(\hat{\mathbf{r}}\cdot\boldsymbol{\sigma}_2) - \boldsymbol{\sigma}_1\cdot\boldsymbol{\sigma}_2\right)e^{i\mathbf{k}\cdot\mathbf{r}}d\mathbf{r} =$$

$$-\left(3(\mathbf{q}\cdot\boldsymbol{\sigma}_1)(\mathbf{q}\cdot\boldsymbol{\sigma}_2) - q^2\boldsymbol{\sigma}_1\cdot\boldsymbol{\sigma}_2\right)\frac{1}{2\pi^2q^2}\int_0^\infty j_2(qr)V(r)r^2dr \tag{1.12}$$

These expressions are used to represent the momentum-space interaction as a sum of scalar functions of $q := |\mathbf{q}|$ multiplied by spin-isospin operators. The scalar functions of momentum transfer that multiply the spin-isospin operators are:

$$\tilde{V}_m(q) = \frac{1}{2\pi^2}\int_0^\infty j_0(qr)V_m(r)r^2dr \qquad m \in \{1,2,3,4,15,16,18\} \tag{1.13}$$

$$\tilde{V}_m(q) = \frac{1}{2\pi^2 q}\int_0^\infty j_1(qr)V_m(r)r^3dr \qquad m \in \{7,8,9b,10b,11b,12b,13b,14b\} \tag{1.14}$$

$$\tilde{V}_m(q) = \frac{1}{2\pi^2 q^2}\int_0^\infty j_2(qr)V_m(r)r^4dr \qquad m \in \{9a,10a,11a,12a,13a,14a\} \tag{1.15}$$

$$\tilde{V}_m(q) = \frac{1}{2\pi^2 q^2}\int_0^\infty j_2(qr)V_m(r)r^2dr \qquad m \in \{5,6,17\} \tag{1.16}$$

where $V_m(r)$ is the m^{th} potential in the expansion (**??**) and $\tilde{V}_{ma}(q)$ and $\tilde{V}_{mb}(q)$ are the two different functions that appear in (**??**) and (**??**). These functions have a finite limit as $q \to 0$ in spite of the $1/q^l$ coefficient because the Bessel function $j_l(qr)$ vanishes like q^l as $q \to 0$.

The resulting momentum-space potential can be expressed as

$$\langle \mathbf{k}'|V|\mathbf{k}\rangle = \sum_{m\in S}\tilde{V}_m(q)\tilde{O}_m \tag{1.17}$$

where $S = \{1,2,3,4,5,6,7,8,9a,9b,10a,10b,11a,11b,12a,12b,13a,13b,14a,14b,15,16,17,18\}$. The 24 operators $\tilde{O}_m$ are

$$\tilde{O}_1 = I \qquad \tilde{O}_2 = (\boldsymbol{\tau}_1\cdot\boldsymbol{\tau}_2) \qquad \tilde{O}_3 = (\boldsymbol{\sigma}_1\cdot\boldsymbol{\sigma}_2) \qquad \tilde{O}_4 = (\boldsymbol{\sigma}_1\cdot\boldsymbol{\sigma}_2)(\boldsymbol{\tau}_1\cdot\boldsymbol{\tau}_2) \tag{1.18}$$

$$\tilde{O}_5 = -\big(3(\mathbf{q}\cdot\boldsymbol{\sigma}_1)(\mathbf{q}\cdot\boldsymbol{\sigma}_2) - q^2\boldsymbol{\sigma}_1\cdot\boldsymbol{\sigma}_2\big) \qquad \tilde{O}_6 = -\big(3(\mathbf{q}\cdot\boldsymbol{\sigma}_1)(\mathbf{q}\cdot\boldsymbol{\sigma}_2) - q^2\boldsymbol{\sigma}_1\cdot\boldsymbol{\sigma}_2\big)(\boldsymbol{\tau}_1\cdot\boldsymbol{\tau}_2) \tag{1.19}$$

$$\tilde{O}_7 = i\mathbf{k}\times\mathbf{k}' \qquad \tilde{O}_8 = i\mathbf{k}\times\mathbf{k}'(\boldsymbol{\tau}_1\cdot\boldsymbol{\tau}_2) \qquad \tilde{O}_{9a} = -(\mathbf{k}'\times\mathbf{k})\cdot(\mathbf{k}'\times\mathbf{k}) \qquad \tilde{O}_{9b} = 2(\mathbf{k}'\cdot\mathbf{k}) \tag{1.20}$$

$$\tilde{O}_{10a} = -(\mathbf{k}'\times\mathbf{k})\cdot(\mathbf{k}'\times\mathbf{k})(\boldsymbol{\tau}_1\cdot\boldsymbol{\tau}_2) \qquad \tilde{O}_{10b} = 2(\mathbf{k}'\cdot\mathbf{k})(\boldsymbol{\tau}_1\cdot\boldsymbol{\tau}_2) \tag{1.21}$$

$$\tilde{O}_{11a} = -(\mathbf{k}'\times\mathbf{k})\cdot(\mathbf{k}'\times\mathbf{k})(\boldsymbol{\sigma}_1\cdot\boldsymbol{\sigma}_2) \qquad \tilde{O}_{11b} = 2(\mathbf{k}'\cdot\mathbf{k})(\boldsymbol{\sigma}_1\cdot\boldsymbol{\sigma}_2) \tag{1.22}$$

$$\tilde{O}_{12a} = -(\mathbf{k}'\times\mathbf{k})\cdot(\mathbf{k}'\times\mathbf{k})(\boldsymbol{\sigma}_1\cdot\boldsymbol{\sigma}_2)(\boldsymbol{\tau}_1\cdot\boldsymbol{\tau}_2) \qquad \tilde{O}_{12b} = 2(\mathbf{k}'\cdot\mathbf{k})(\boldsymbol{\sigma}_1\cdot\boldsymbol{\sigma}_2)(\boldsymbol{\tau}_1\cdot\boldsymbol{\tau}_2) \tag{1.23}$$

$$\tilde{O}_{13a} = -(\mathbf{S}\cdot(\mathbf{k}\times\mathbf{k}'))^2 \qquad \tilde{O}_{13b} = (\mathbf{k}'\times\mathbf{S})\cdot(\mathbf{k}\times\mathbf{S}) \qquad \tilde{O}_{14a} = -(\mathbf{S}\cdot(\mathbf{k}\times\mathbf{k}'))^2(\boldsymbol{\tau}_1\cdot\boldsymbol{\tau}_2) \tag{1.24}$$

$$\tilde{O}_{14b} = (\mathbf{k}'\times\mathbf{S})\cdot(\mathbf{k}\times\mathbf{S})(\boldsymbol{\tau}_1\cdot\boldsymbol{\tau}_2) \qquad \tilde{O}_{15} = T_{12} \qquad \tilde{O}_{16} = (\boldsymbol{\sigma}_1\cdot\boldsymbol{\sigma}_2)T_{12} \tag{1.25}$$

$$\tilde{O}_{17} = -\big(3(\mathbf{q}\cdot\boldsymbol{\sigma}_1)(\mathbf{q}\cdot\boldsymbol{\sigma}_2) - q^2\boldsymbol{\sigma}_1\cdot\boldsymbol{\sigma}_2\big)T_{12} \qquad \tilde{O}_{18} = (\tau_{1z}+\tau_{2z}). \tag{1.26}$$

In the approximate potentials the coefficient functions $\tilde{V}_m(q)$ are replaced by expansions in known functions.

II. EXPANSIONS

Two approaches are used to compute the scalar functions (**??**-**??**). Both approaches involve approximating these functions by a finite linear combination of elementary functions. The first method approximates these functions by linear combinations of Chebyshev polynomials on three distinct intervals of momenta, for momenta up to $100 fm^{-1}$. The second approach approximates the integrand by a finite linear combination of orthogonal functions that have analytic Fourier transforms. The configuration-space basis functions are associated Laguerre polynomials multiplied by decaying exponentials which have analytic Fourier transforms that can be expressed in terms of Jacobi polynomials [**?**]. In both approaches the coefficients of the expansion are stored and the potentials can then be efficiently computed for any values of momenta by summing a finite series of elementary functions. In both cases the required expansion functions at any point can be determined recursively, leading to efficient and accurate approximations to the momentum space potential.

This section discusses the Chebyshev basis. Because the configuration space potential falls off asymptotically like $e^{-m_\pi r}$, the radial integrals are evaluated with a finite cutoff at 20 fm. The Chebyshev expansion is used for $q < 100\, fm^{-1}$. With these cutoffs the maximum value of $x := qr$ that can appear in the argument of the spherical Bessel functions in the integrals (**??**-**??**) is $x_{max} = 2000$. To evaluate these integrals the zeros of the spherical Bessel functions $j_0(x)$, $j_1(x)$, and $j_2(x)$ for $0 \leq x \leq 2000$ are computed for each fixed value of q. For each value of q the integrals are expressed as sums integrals between successive zeros of the spherical Bessel function that appear in the integral. If q is such that qr is never a zero of $j_l(qr)$ for $0 < r < 20 fm$ then the integral over r is performed using a 100 point Gauss-Legendre quadrature on the interval $[0, 20 fm]$. If q is such that qr has zeros of $j_l(qr)$ for $0 < r < 20 fm$, then the integrals between zeros $[qr_i, qr_{i+1}]$ are computed using 20 Gauss-Legendre points when $r_{i+1} \leq 5\, fm$, 40 Gauss-Legendre points when $5\, fm < r_{i+1} \leq 10\, fm$ and 80 Gauss-Legendre points when $10\, fm < r_{i+1} \leq 20\, fm$.

The functions $\tilde{V}_m(q)$ are replaced by a Chebyshev polynomial approximation on the interval $q \in [a, b]$ using [**?**]

$$\tilde{V}_m(q) \approx c_0/2 + \sum_{n=1}^{100} c_n T_n\left(-\frac{a+b}{b-a} + \frac{2}{b-a} q\right) \tag{2.1}$$

where

$$T_n(x) = \cos(n \cos^{-1}(x))) \tag{2.2}$$

are Chebyshev polynomials and the coefficients c_n are computed using a Clenshaw-Curtiss quadrature[**?**] :

$$c_n = \frac{2}{N}[\frac{1}{2}\tilde{V}_m(b) + \sum_{j=1}^{N-1} \tilde{V}_m(\frac{a+b}{2} + \frac{b-a}{2}\cos(\pi j/N))\cos(nj\pi/N) + (-)^n \frac{1}{2}\tilde{V}_m(a)] \tag{2.3}$$

with $N = 101$. The functions $\tilde{V}_m(q)$ are evaluated at the quadrature points $q_j := \frac{a+b}{2} + \frac{b-a}{2}\cos(\pi j/N)$ using the methods discussed above. This is repeated for q in each of three intervals, $[a, b] = [0, 10], [10, 50], [50, 100]$ and the 101 expansion coefficients associated with each of these three intervals are stored. The Chebyshev polynomials are computed using the recurrence relations

$$T_{n+1}(x) = 2xT_n(x) - T_{n-1}(x), \qquad T_0(x) = 1,\, T_1(x) = x. \tag{2.4}$$

For q larger than 100 fm^{-1} $\tilde{V}_m(q)$ is approximated by 0.

This method provides an accurate and efficient representation for computing a momentum space $V18$ interaction. While it requires a substantial effort to compute the integrals at the required quadrature points, this only has to be done once.

III. BASIS FUNCTIONS

While the method of the previous section gives accurate results, a more straightforward approach is to represent the potential directly as an expansion in basis functions that have analytic Fourier transforms. The plots in figures 1-24 show the configuration-space functions that must be Fourier-Bessel transformed for each of the 24 integrals listed in (**??**-**??**). These graphs actually show both the exact radial functions and the basis function expansions of these functions, which are discussed below. The curves are indistinguishable on these plots. The plots show that the radial functions are simple smooth functions.

In order to represent the potential, each of the scalar potentials $\tilde{V}_m(q)$, is approximated by an expansion in known basis functions. A method to compute both the expansion coefficients and a recursion formula to compute basis functions are given below.

The functions $V_m(r)$, $rV_m(r)$, and $r^2V_m(r)$ that appear in the integrals (**??**-**??**) are expanded using an orthonormal set of radial functions that have analytic Fourier-Bessel transforms [**?**]. These functions are associated Laguerre polynomials multiplied by decaying exponentials in configuration space. Their Fourier-Bessel transforms have power-law fall of in momentum space. In addition, they vanish at the origin in a manner that can be used to explicitly cancel the factors $1/q$ and $1/q^2$ that appear in the definitions (**??**-**??**) of $\tilde{V}_m$. Both sets of basis functions can be generated efficiently using recursion relations. The cancellation of the factors $1/q$ and $1/q^2$ can be directly incorporated into the recursion that generates the momentum-space basis functions so the final expression for the potential does not require a special treatment for q near 0.

The radial basis functions for different values of l are given below. The dimensionless parameter $x := \Lambda r$ is used in the basis functions, where Λ is a scale parameter that can be chosen to improve convergence. The parameterization of the Argonne V18 interaction uses the value $\Lambda = 7(fm)^{-1}$. The configuration space basis functions are

$$\phi_{nl}(r) = \frac{1}{\sqrt{N_{nl}}} x^l L_n^{2l+2}(2x)e^{-x} \tag{3.1}$$

where

$$L_n^{\alpha} = \sum_{m=0}^{n} (-)^m \begin{pmatrix} n+\alpha \\ n-m \end{pmatrix} \frac{x^m}{m!} \tag{3.2}$$

and the normalization coefficient is

$$N_{nl} = \Lambda^{-3}(\frac{1}{2})^{2l+3} \frac{\Gamma(n+\alpha+1)}{n!}. \tag{3.3}$$

These functions satisfy the orthogonality relations

$$\int_0^\infty \phi_{nl}(r)\phi_{ml}(r) r^2 dr = \delta_{mn}. \tag{3.4}$$

They have analytic Fourier-Bessel transforms defined by

$$\tilde{\phi}_{nl}(q) = \sqrt{\frac{2}{\pi}} \int_0^\infty j_l(qr)\phi_{nl}(r) r^2 dr. \tag{3.5}$$

For $y = q/\Lambda$ the $\tilde{\phi}_{nl}(q)$ can be expressed in terms of Jacobi polynomials:

$$\tilde{\phi}_{nl}(q) = \frac{1}{\sqrt{\tilde{N}_{nl}}} \frac{y^l}{(y^2+1)^{l+2}} P_n^{l+\frac{3}{2},l+\frac{1}{2}}(\frac{y^2-1}{y^2+1}) \tag{3.6}$$

with normalization coefficient

$$\tilde{N}_{nl} = \frac{\Lambda^3}{2(2n+2l+3)} \frac{\Gamma(n+l+\frac{5}{2})\Gamma(n+l+\frac{3}{2})}{n!\Gamma(n+2l+3)} \tag{3.7}$$

and

$$P_n^{(\alpha,\beta)}(z) = \frac{\Gamma(\alpha+n+1)}{n!\Gamma(\alpha+\beta+n+1)} \sum_{m=0}^{n} \begin{pmatrix} n \\ m \end{pmatrix} \frac{\Gamma(\alpha+\beta+n+m+1)}{2^m\Gamma(\alpha+m+1)}(z-1)^m. \tag{3.8}$$

These functions satisfy the orthogonality relations

$$\int_0^\infty \tilde{\phi}_{nl}(q)\tilde{\phi}_{ml}(q)q^2dq = \delta_{mn}. \tag{3.9}$$

These basis functions can be generated by using the following recursion formulas for the associated Laguerre functions and Jacobi polynomials

$$(n+1)L_{n+1}^\alpha(x) = (2n+\alpha+1-x)L_{n+}^\alpha(x) - (n+\alpha)L_{n-1}^\alpha(x) \tag{3.10}$$

and

$$\begin{gathered} 2(n+1)(n+\alpha+\beta+1)(2n+\alpha+\beta)P_{n+1}^{(\alpha,\beta)}(x) = \\ [(2n+\alpha+\beta+1)(\alpha^2-\beta^2)+x((2n+\alpha+\beta)(2n+\alpha+\beta+1)(2n+\alpha+\beta+2)]P_n^{(\alpha,\beta)}(x) \\ -2(n+\alpha)(n+\beta)(2n+\alpha+\beta+2)P_{n-1}^{(\alpha,\beta)}(x). \end{gathered} \tag{3.11}$$

These recursion relations can be modified to incorporate the normalization constants (**??**) and (**??**) directly into the recursion. The recursion for the normalized radial basis functions with ($x = \Lambda r$) is given by:

$$\phi_{0l}(r) = \frac{1}{\sqrt{(2*l+1)!}} \frac{1}{\sqrt{2^{2l+3}}} \Lambda^{3/2} x^l e^{-x} \tag{3.12}$$

$$\phi_{1l}(r) = \frac{2l+3-2x}{\sqrt{2l+3}} \phi_{0l}(r) \tag{3.13}$$

$$\phi_{nl}(r) = \frac{2n+1+2l-2x}{\sqrt{n+1+2l}\sqrt{n}} \phi_{n-1,l}(r) - \sqrt{\frac{(n-1)(n+1+2l)}{n(n+2+2l)}} \phi_{n-2,l}(r) \tag{3.14}$$

Similarly, the normalized momentum-space basis functions with ($y = q/\Lambda$) are generated by the recursion:

$$\begin{gathered} \tilde{\phi}_{0l}(q) = \\ \frac{1}{\sqrt{(2l+3)!}} \frac{1}{\sqrt{\Lambda^3}} \frac{1}{\sqrt{\frac{1}{2}\cdots\frac{2l+3}{2}}} \frac{1}{\sqrt{\frac{1}{2}\cdots\frac{2l+1}{2}}} y^l \frac{1}{(y^2+1)^{2l+2}} \end{gathered} \tag{3.15}$$

$$\tilde{\phi}_{1l}(q) = (\frac{1}{2} + (l+2)\frac{y^2-1}{y^2+1})\sqrt{\frac{2l+5}{(l+2+\frac{1}{2})(l+1+\frac{1}{2})}}\tilde{\phi}_{0l}(q) \tag{3.16}$$

$$\begin{aligned}
&\tilde{\phi}_{nl}(q) = \\
&\sqrt{\frac{(2n+2l+3)n(n+2l+2)}{(2n+2l+1)(n+l+\frac{3}{2})(n+l+\frac{1}{2})}} \\
&\times\frac{(2n+2l+1)(2l+2)(y^2+1)+(2n+2l+1)(2n+2l)(2n+2l+2)(y^2-1)}{2n(n+2l+2)(2n+2l)(y^2-1)}\tilde{\phi}_{n-1l}(q) \\
&-\sqrt{\frac{(2n+2l+3)(n-1)n(n+1+2l)(n+2l+2)}{(2n+2l-1)(n+l+\frac{3}{2})(n+l+\frac{1}{2})(n+l+\frac{1}{2})(n+l-\frac{1}{2})}} \\
&\times\frac{(n+l+\frac{1}{2})(n+l-\frac{1}{2})(2n+2l+2)}{(n)(n+2l+2)(2n+2l)}\tilde{\phi}_{n-1l}(q).
\end{aligned} \tag{3.17}$$

Replacing $\tilde{\phi}_{0l}(q)$ by $\hat{\phi}_{0l}(q) := \tilde{\phi}_{0l}(q)/q^l$ given by

$$\begin{aligned}
&\hat{\phi}_{0l}(q) = \\
&\frac{1}{\sqrt{(2l+3)!}}\frac{1}{\sqrt{\Lambda^3}}\frac{1}{\sqrt{\frac{1}{2}\cdots\frac{2l+3}{2}}}\frac{1}{\sqrt{\frac{1}{2}\cdots\frac{2l+1}{2}}}\Lambda^{-l}\frac{1}{(y^2+1)^{2l+2}}
\end{aligned} \tag{3.18}$$

to start the recursion in equations (**??**)-(**??**) generates $\hat{\phi}_{nl}(q) := \tilde{\phi}_{nl}(q)/q^l$, which are well-behaved as $q \to 0$. Seventy expansion coefficients are used to construct the momentum-space potential for each value of m

$$c_{nm} = \frac{1}{2\pi^2}\int_0^\infty \phi_{n0}(r)V_m(r)r^2dr \qquad m \in \{1,2,3,4,15,16,18\} \tag{3.19}$$

$$c_{nm} = \frac{1}{2\pi^2}\int_0^\infty \phi_{n1}(r)V_m(r)r^3dr \qquad m \in \{7,8,9b,10b,11b,12b,13b,14b\} \tag{3.20}$$

$$c_{nm} = \frac{1}{2\pi^2}\int_0^\infty \phi_{n2}(r)V_m(r)r^4dr \qquad m \in \{9a,10a,11a,12a,13a,14a\} \tag{3.21}$$

$$c_{nm} = \frac{1}{2\pi^2}\int_0^\infty \phi_{n2}(r)V_m(r)r^2dr \qquad m \in \{5,6,17\} \tag{3.22}$$

The integrals are approximated using an 80 point Gauss Legendre quadrature between 0 and $10fm$. The basis functions $\phi_{nl}(r)$ are generated using (**??-??**). The scale parameter in the recursion for $\phi_{nl}(r)$ is taken as $\Lambda = 7fm^{-1}$.

The 70x24 expansion coefficients c_{nm} are stored. The momentum space potential functions are then given by

$$\tilde{V}_m(q) = \sum_{n=1}^{70} c_{nm}\hat{\phi}_{nl}(q) \tag{3.23}$$

where the reduced expansion functions $\hat{\phi}_{nl}(q) := \tilde{\phi}_{nl}(q)/q^l$ are generated recursively using (??-??).

The full momentum-space potential in operator form is given by

$$V = \sum_{m \in S} \tilde{V}_m(q)\tilde{O}_m \tag{3.24}$$

where $\tilde{O}_m$ are the 24 operators (??-??) and $q = \sqrt{k^2 + k'^2 - 2\mathbf{k}' \cdot \mathbf{k}}$.

IV. TESTS

Three tests are performed on the two potentials. First, the exact radial functions that appear on the right side of the integrals (??-??) are compared with their configuration space expansions in the basis (??). Second, the momentum space coefficient functions, $\tilde{V}_m(q)$ are compared to the more precise calculation of the Fourier-Bessel transforms based on direct Fourier-Bessel transforms with a Chebyshev polynomial interpolation. Finally, both potentials are used to compute the deuteron binding energy and wave functions. These results are compared to a direct calculation of these quantities using the partial wave expansion of the original configuration space potential.

Figures 1-24 compare the structure of the 24 configuration space functions (the integrands in (??-??) for $r < 5fm$ computed from the 70 term expansion (dashed lines) to the exact expressions (solid lines). The difference between the exact and approximate radial functions is too small to be seen in these plots. The quality of the approximations is not surprising given that exact functions are smooth with minimal structure.

To test the Fourier transforms the Fourier-Bessel transforms (??-??) based on the Chebyshev expansion, discussed in the previous section, are compared to the Fourier-Bessel transforms obtained by analytically Fourier transforming the basis functions. Figures 25-48 show both plots. The solid lines are the series expansions while the dashed lines are the Chebyshev expansion. The figures for the potentials associated with the

Again differences are not visible on these plots. A better comparison is given in tables 1-4, which list values of the Fourier-Bessel transforms of the 24 radial functions using both methods for momenta of 1,5,15 and 25 fm^{-1}.

Table 1. - Fourier transforms at 1 fm^{-1}

n	series	Chebyshev expansion
1	6.789973e-01	6.789990e-01
2	-4.019392e-01	-4.019400e-01
3	-1.692090e-01	-1.692090e-01
4	2.358519e-01	2.356720e-01
5	7.216739e-03	7.218230e-03
6	2.857732e-01	2.860470e-01
7	-5.511547e-01	-5.511560e-01
8	-1.678888e-01	-1.678890e-01
9	1.741415e-01	1.741420e-01
10	-3.272988e-02	-3.272990e-02
11	1.999136e-02	1.999140e-02
12	-7.414060e-03	-7.414070e-03
13	9.084422e-02	9.084440e-02
14	1.245017e-01	1.245020e-01
15	1.122388e-02	1.122390e-02
16	-1.214926e-02	-1.216020e-02
17	2.403290e-03	2.420790e-03
18	6.124964e-03	6.124970e-03
19	1.304278e-02	1.304280e-02
20	-1.702409e-02	-1.702400e-02
21	-7.227244e-03	-7.227270e-03
22	-7.849686e-03	-7.849720e-03
23	4.518193e-02	4.518270e-02
24	3.980251e-02	3.980280e-02

Table 2. - Fourier transforms at 5 fm^{-1}

n	series	Chebyshev expansion
1	1.160699e+00	1.160700e+00
2	-1.360382e-02	-1.360380e-02
3	-1.148807e-01	-1.148810e-01
4	-1.065288e-01	-1.065200e-01
5	4.489757e-03	4.489760e-03
6	4.405849e-03	4.405360e-03
7	-4.623736e-02	-4.623740e-02
8	-1.871380e-02	-1.871380e-02
9	2.471311e-02	2.471320e-02
10	1.480758e-03	1.480760e-03
11	6.027203e-03	6.027210e-03
12	1.465070e-03	1.465070e-03
13	5.222260e-03	5.222270e-03
14	8.233502e-03	8.233520e-03
15	4.828280e-03	4.828290e-03
16	-4.815794e-03	-4.815310e-03
17	1.656921e-06	1.627536e-06
18	4.274306e-04	4.274310e-04
19	4.273833e-03	4.273840e-03
20	1.791462e-04	1.791460e-04
21	9.672551e-04	9.672570e-04
22	1.814761e-04	1.814760e-04
23	1.620319e-03	1.620320e-03
24	1.790086e-03	1.790090e-03

Table 3. - Fourier transforms at 15 fm^{-1}

n	series	Chebyshev expansion
1	9.321365e-04	9.321050e-04
2	4.123439e-05	4.123390e-05
3	-1.924812e-05	-1.924670e-05
4	-6.648375e-05	-6.643920e-05
5	-9.010902e-06	-9.010533e-06
6	1.026393e-05	1.026324e-05
7	5.541260e-06	5.540870e-06
8	2.632043e-06	2.631910e-06
9	-1.962835e-06	-1.962590e-06
10	-9.304609e-07	-9.304860e-07
11	-6.015901e-07	-6.015370e-07
12	-1.047669e-07	-1.047530e-07
13	-4.725022e-06	-4.725160e-06
14	-1.527634e-06	-1.527590e-06
15	2.942747e-06	2.942630e-06
16	-2.895027e-06	-2.892440e-06
17	-2.865458e-10	-3.050827e-10
18	9.986465e-08	9.985120e-08
19	-2.604487e-07	-2.604660e-07
20	-6.335039e-08	-6.334960e-08
21	-7.055132e-08	-7.055530e-08
22	-1.454468e-08	-1.454570e-08
23	-3.115148e-07	-3.115090e-07
24	-1.394089e-07	-1.394130e-07

Table 4. - Fourier transforms at 25 fm^{-1}

n	series	Chebyshev expansion
1	-1.386301e-05	-1.383430e-05
2	-6.108349e-08	-6.010020e-08
3	8.598072e-07	8.595170e-07
4	1.014189e-06	1.003920e-06
5	-4.600082e-07	-4.599216e-07
6	4.739733e-07	4.738720e-07
7	2.443040e-08	2.442090e-08
8	9.428095e-09	9.412980e-09
9	-1.534834e-08	-1.533920e-08
10	3.457372e-10	3.607580e-10
11	-3.619628e-09	-3.613210e-09
12	-1.005784e-09	-1.003140e-09
13	4.666338e-09	4.709400e-09
14	-3.274714e-09	-3.270330e-09
15	-5.425469e-08	-5.415690e-08
16	5.452722e-08	5.399650e-08
17	-2.888773e-12	-4.234000e-12
18	-5.852151e-09	-5.841450e-09
19	-2.512190e-10	-2.555620e-10
20	7.827015e-12	7.411800e-12
21	-5.864134e-11	-5.980770e-11
22	-1.617550e-11	-1.652710e-11
23	8.297311e-11	8.271960e-11
24	-5.322500e-11	-5.424550e-11

Table 5 s and d wave functions using Chebyshev, series and partial waves

kfm^{-1}	s-Cheb.	s-pw	s-series	d-Cheb,	d-pw	d-series
0.0	1.2695e+01	1.2638e+01	1.2695e+01	0.00000e+00	0.00000e+00	0.00000e+00
0.5	1.9609e+00	1.9606e+00	1.9609e+00	-2.19827e-01	-2.19752e-01	-2.19811e-01
1.0	3.7684e-01	3.7687e-01	3.7685e-01	-1.72164e-01	-1.72174e-01	-1.7216e-01
1.5	8.2472e-02	8.2472e-02	8.2473e-02	-1.1243e-01	-1.12418e-01	-1.1243e-01
2.0	6.0810e-03	6.1039e-03	6.0810e-03	-7.10859e-02	-7.10846e-02	-7.10868e-02
2.5	-1.3615e-02	-1.3601e-02	-1.3616e-02	-4.4543e-02	-4.45444e-02	-4.45435e-02
3.0	-1.6153e-02	-1.6154e-02	-1.6153e-02	-2.76854e-02	-2.76819e-02	-2.76856e-01
3.5	-1.3648e-02	-1.3648e-02	-1.3648e-02	-1.69881e-02	-1.69856e-02	-1.69882e-02
4.0	-1.0153e-02	-1.0146e-02	-1.0153e-02	-1.02234e-02	-1.02219e-02	-1.02235e-02
4.5	-6.9954e-03	-6.9994e-03	-6.9955e-03	-5.98474e-03	-5.98642e-03	-5.9848e-03
5.0	-4.5270e-03	-4.5234e-03	-4.5271e-03	-3.37042e-03	-3.36900e-03	-3.37046e-03

As a final test the deuteron binding energy and wave functions using the two different momentum space potentials are compared to each other and to the same quantities using a direct calculation based on the configuration space potential in partial waves.

We solve for the deuteron binding energy and the s and d wave functions using direct integration of the vector variables. The method of solution, which is discussed in [?], uses the expansion (??) directly without using partial waves. Calculations are performed for both momentum space potentials.

For comparison, the wave functions are represented by an expansion in 70 configuration space basis using the configuration space basis functions (??). Matrix elements of the partial wave projection of the Hamiltonian in this basis are directly computed and the eigenvalue problem is solved. The solution of the eigenvalue problem gives an independent evaluation of both the binding energy and wave functions that do not require Fourier transforms of the potential.

The Deuteron binding energy obtained by both Fourier transform methods was $e = -2.24225 MeV$ compared with $e = -2.24221 MeV$ using a partial wave calculation that directly uses the configuration space version of the Argonne V18 potential. These eigenvalues differ slightly from the eigenvalues obtained including the electromagnetic corrections of +17.6 keV [?]. If this correction is added to the numbers above the binding energy $e = -2.2246 MeV$, is obtained.

The s and d wave functions for all three calculations are shown in figures 49 and 50. The solid lines represent the wave functions computed using the Chebyshev expansion of the Fourier transformed potential, the long dashes represent the partial wave wave-functions and the short dashes represent the wave functions computed using the series expansion of the Fourier transformed potential. Explicit values of both wave functions in all three calculations are compared table 5. The wave functions differ in the fourth significant figure for momenta less that 5 fm^{-1}, while binding energies of all three calculations differ in the seventh significant figure. This level of accuracy should be adequate for most applications.

The programs to compute the potentials $\tilde{V}_m(q)$ are freely available as supplementary material to the electronic version of this article.

This work supported by the U.S. Department of Energy, contract # DE-FG02-86ER40286.

V. APPENDIX

In this appendix we calculate the Fourier transform of the operators that appear (**??**-**??**) in V18.

$\mathbf{L}\cdot\mathbf{S}$: Let $\mathbf{q}=\mathbf{k}-\mathbf{k}'$

$$\frac{1}{(2\pi)^3}\int e^{-i\mathbf{k}'\cdot\mathbf{r}}V_j(r)\mathbf{L}\cdot\mathbf{S}e^{i\mathbf{k}\cdot\mathbf{r}}d\mathbf{r}=\frac{1}{(2\pi)^3}\int e^{-i\mathbf{k}'\cdot\mathbf{r}}V_j(r)\mathbf{S}\cdot(\mathbf{r}\times\mathbf{p})e^{i\mathbf{k}\cdot\mathbf{r}}d\mathbf{r}=$$
$$\frac{1}{(2\pi)^3}\int e^{-i\mathbf{k}'\cdot\mathbf{r}}V_j(r)\mathbf{S}\cdot(\mathbf{r}\times\mathbf{k})e^{i\mathbf{k}\cdot\mathbf{r}}d\mathbf{r}=\frac{1}{(2\pi)^3}\int e^{i\mathbf{q}\cdot\mathbf{r}}V_j(r)\mathbf{S}\cdot(\mathbf{r}\times\mathbf{k})d\mathbf{r}=$$
$$\frac{4\pi}{(2\pi)^3}\int\sum_{l=0}^{\infty}\sum_{m=-l}^{l}i^l j_l(qr)Y_{lm}(\hat{\mathbf{q}})Y_{lm}^*(\hat{\mathbf{r}})V_j(r)\mathbf{S}\cdot(\mathbf{r}\times\mathbf{k})d\mathbf{r}. \tag{5.1}$$

Since $\mathbf{r}$ can be expanded as a linear combination of $Y_{1m}(\hat{\mathbf{r}})$ the only terms that survive are the $l=1$ terms. The integral over angles and the spherical harmonics simply replace $\hat{\mathbf{r}}$ by $\hat{\mathbf{q}}$, giving

$$=\frac{4\pi i}{(2\pi)^3}\int_0^\infty j_1(qr)V_j(r)\mathbf{S}\cdot(\mathbf{q}\times\mathbf{k})r^3dr=\mathbf{S}\cdot(\mathbf{k}\times\mathbf{k}')\times[\frac{4\pi i}{q(2\pi)^3}\int_0^\infty j_1(qr)V_j(r)r^3dr]=$$
$$\mathbf{S}\cdot(\mathbf{k}\times\mathbf{k}')\times[\frac{i}{2\pi^2 q}\int_0^\infty j_1(qr)V_j(r)r^3dr] \tag{5.2}$$

Thus we get

$$\frac{1}{(2\pi)^3}\int e^{-i\mathbf{k}'\cdot\mathbf{r}}V_j(r)\mathbf{L}\cdot\mathbf{S}e^{i\mathbf{k}\cdot\mathbf{r}}d\mathbf{r}=i\mathbf{S}\cdot(\mathbf{k}\times\mathbf{k}')I_1(q) \tag{5.3}$$

where

$$I_1(q) := \frac{1}{2\pi^2 q} \int_0^\infty j_1(qr) V_j(r) r^3 dr \tag{5.4}$$

The following relations are useful for treating the remaining three operators:

$$\boldsymbol{\nabla}_q f(q) = f'(q)\frac{\mathbf{q}}{q} \tag{5.5}$$

$$\nabla_q^2 f(q) = f''(q) + f'(q)\frac{3}{q} - f'(q)\frac{1}{q} = f''(q) + \frac{2}{q}f'(q) \tag{5.6}$$

$$(\mathbf{a}\cdot\boldsymbol{\nabla}_q)(\mathbf{b}\cdot\boldsymbol{\nabla}_q) f(q) = f''(q)\frac{\mathbf{a}\cdot\mathbf{q}}{q}\frac{\mathbf{b}\cdot\mathbf{q}}{q} + f'(q)\frac{\mathbf{a}\cdot\mathbf{b}}{q} - f'(q)\frac{(\mathbf{a}\cdot\mathbf{q})(\mathbf{b}\cdot\mathbf{q})}{q^3} = \tag{5.7}$$

$$\frac{\mathbf{a}\cdot\mathbf{q}}{q}\frac{\mathbf{b}\cdot\mathbf{q}}{q}((f''(q) - \frac{f'(q)}{q}) + \frac{\mathbf{a}\cdot\mathbf{b}}{q}f'(q) \tag{5.8}$$

$\mathbf{L}\cdot\mathbf{L}$: Let $\mathbf{q} = \mathbf{k} - \mathbf{k}'$

$$\frac{1}{(2\pi)^3}\int e^{-i\mathbf{k}'\cdot\mathbf{r}} V_j(r)(\mathbf{r}\times\mathbf{p})\cdot(\mathbf{r}\times\mathbf{p}) e^{i\mathbf{k}\cdot\mathbf{r}} d\mathbf{r} = \frac{1}{(2\pi)^3}\int e^{-i\mathbf{k}'\cdot\mathbf{r}} V_j(r)(\mathbf{r}\times\mathbf{k}')\cdot(\mathbf{r}\times\mathbf{k}) e^{i\mathbf{k}\cdot\mathbf{r}} d\mathbf{r} =$$

$$(-i\boldsymbol{\nabla}_q\times\mathbf{k}')\cdot(-i\boldsymbol{\nabla}_q\times\mathbf{k})\frac{1}{(2\pi)^3}\int V_j(r) e^{i\mathbf{q}\cdot\mathbf{r}} d\mathbf{r} = -(\boldsymbol{\nabla}_q\times\mathbf{k}')\cdot(\boldsymbol{\nabla}_q\times\mathbf{k})\frac{4\pi}{(2\pi)^3}\int_0^\infty V_j(r) j_0(qr) r^2 dr. \tag{5.9}$$

To compute the derivatives note

$$(\boldsymbol{\nabla}_q\times\mathbf{k}')\cdot(\boldsymbol{\nabla}_q\times\mathbf{k}) =$$

$$(\mathbf{k}\cdot\mathbf{k}')(\boldsymbol{\nabla}_q\cdot\boldsymbol{\nabla}_q) - (\mathbf{k}\cdot\boldsymbol{\nabla}_q)(\mathbf{k}\cdot\boldsymbol{\nabla}_q)$$

Using this in the above gives

$$-(\boldsymbol{\nabla}_q\times\mathbf{k}')\cdot(\boldsymbol{\nabla}_q\times\mathbf{k})\frac{4\pi}{(2\pi)^3}\int_0^\infty V_j(r) j_0(qr) r^2 dr = -\left((\mathbf{k}'\cdot\mathbf{k})\nabla_q^2 - (\mathbf{k}'\cdot\boldsymbol{\nabla}_q)(\mathbf{k}\cdot\boldsymbol{\nabla}_q)\right) I_0(q) \tag{5.10}$$

where

$$I_0(q) = \frac{4\pi}{(2\pi)^3}\int_0^\infty V_j(r) j_0(qr) r^2 dr = \frac{1}{2\pi^2}\int_0^\infty V_j(r) j_0(qr) r^2 dr \tag{5.11}$$

Evaluating this gives

$$-\left((\mathbf{k}'\cdot\mathbf{k})\nabla_q^2 - (\mathbf{k}'\cdot\boldsymbol{\nabla}_q)(\mathbf{k}\cdot\boldsymbol{\nabla}_q)\right) I_0(q) =$$

$$-(\mathbf{k}'\cdot\mathbf{k})(I_0''(q) + \frac{2}{q}I_0'(q)) + I_0'(q)(\frac{\mathbf{k}'\cdot\mathbf{k}}{q} - \frac{(\mathbf{k}'\cdot\mathbf{q})(\mathbf{k}\cdot\mathbf{q})}{q^3}) + I_0''(q)\frac{(\mathbf{k}'\cdot\mathbf{q})(\mathbf{k}\cdot\mathbf{q})}{q^2} =$$

$$-(\mathbf{k}'\cdot\mathbf{k})(I_0''(q)+\frac{1}{q}I_0'(q))+\frac{(\mathbf{k}'\cdot\mathbf{q})(\mathbf{k}\cdot\mathbf{q})}{q^2}(I_0''(q)-\frac{1}{q}I_0'(q)) \tag{5.12}$$

To eliminate the derivatives use

$$I_0''(q)-\frac{1}{q}I_0'(q)=\frac{1}{2\pi^2}\int_0^\infty V(r)(j_0''(qr)r^2-j_0'(qr)\frac{r}{q})r^2dr=$$

$$\frac{1}{2\pi^2}\int_0^\infty V(r)(j_0''(qr)-j_0'(qr)\frac{1}{qr})r^4dr=\frac{1}{2\pi^2}\int_0^\infty V(r)j_2(qr)r^4dr=I_2(q)$$

$$I_0''(q)+\frac{1}{q}I_0'(q)=\frac{1}{2\pi^2}\int_0^\infty V(r)(j_0''(qr)-j_0'(qr)\frac{1}{qr}+2j_0'(qr)\frac{1}{qr})r^4dr=$$

$$\frac{1}{2\pi^2}\int_0^\infty V(r)j_2''(qr)r^4dr-\frac{1}{2\pi^2}\frac{2}{q}\int_0^\infty V(r)j_1(qr)r^3dr=I_2(q)-\frac{2}{q}I_1(q)$$

This gives

$$\frac{1}{(2\pi)^3}\int e^{-i\mathbf{k}'\cdot\mathbf{r}}V_j(r)(\mathbf{r}\times\mathbf{p})\cdot(\mathbf{r}\times\mathbf{p})e^{i\mathbf{k}\cdot\mathbf{r}}d\mathbf{r}=-(\mathbf{k}'\cdot\mathbf{k})(I_2(q)-\frac{2}{q}I_1(q))+\frac{(\mathbf{k}'\cdot\mathbf{q})(\mathbf{k}\cdot\mathbf{q})}{q^2}I_2(q) \tag{5.13}$$

which can be reexpressed in terms of cross products

$$\frac{1}{(2\pi)^3}\int e^{-i\mathbf{k}'\cdot\mathbf{r}}V_j(r)(\mathbf{r}\times\mathbf{p})\cdot(\mathbf{r}\times\mathbf{p})e^{i\mathbf{k}\cdot\mathbf{r}}d\mathbf{r}=-I_2(q)\frac{(\mathbf{k}'\times\mathbf{k})\cdot(\mathbf{k}'\times\mathbf{k})}{q^2}+\frac{2}{q}(\mathbf{k}'\cdot\mathbf{k})I_1(q) \tag{5.14}$$

$(\mathbf{L}\cdot\mathbf{S})^2$:

$$\frac{1}{(2\pi)^3}\int e^{-i(\mathbf{k}'-\mathbf{k})\cdot\mathbf{r}}V_j(r)(\mathbf{L}\cdot\mathbf{S})^2d\mathbf{r}=\frac{1}{(2\pi)^3}\int e^{-i(\mathbf{k}'-\mathbf{k})\cdot\mathbf{r}}V_j(r)(\mathbf{S}\cdot(\mathbf{r}\times\mathbf{p}))^2d\mathbf{r}=$$

$$-\frac{4\pi}{(2\pi)^3}((\mathbf{k}'\times\mathbf{S})\cdot\boldsymbol{\nabla}_q)((\mathbf{k}\times\mathbf{S})\cdot\boldsymbol{\nabla}_q)\int j_0(qr)V_j(r)r^2dr=$$

$$-((\mathbf{k}'\times\mathbf{S})\cdot\boldsymbol{\nabla}_q)((\mathbf{k}\times\mathbf{S})\cdot\boldsymbol{\nabla}_q)I_0(q)=$$

$$-((\mathbf{k}'\times\mathbf{S})\cdot\mathbf{q}((\mathbf{k}\times\mathbf{S})\cdot\mathbf{q}))\frac{1}{q^2}(I_0''(q)-\frac{1}{q}I_0'(q))-(\mathbf{k}'\times\mathbf{S})\cdot(\mathbf{k}\times\mathbf{S})\frac{1}{q}I_0'(q)=$$

$$-((\mathbf{k}'\times\mathbf{S})\cdot\mathbf{q}((\mathbf{k}\times\mathbf{S})\cdot\mathbf{q}))=\frac{1}{q^2}I_2(q)+(\mathbf{k}'\times\mathbf{S})\cdot(\mathbf{k}\times\mathbf{S})\frac{1}{q}I_1(q) \tag{5.15}$$

which gives

$$-((\mathbf{S}\cdot(\mathbf{k}\times\mathbf{k}'))^2\frac{1}{q^2}I_2(q)+(\mathbf{k}'\times\mathbf{S})\cdot(\mathbf{k}\times\mathbf{S})\frac{1}{q}I_1(q) \tag{5.16}$$

or

$$\frac{1}{(2\pi)^2}\int e^{-i(\mathbf{k}'-\mathbf{k})}V_j(r)(\mathbf{L}\cdot\mathbf{S})^2d\mathbf{r}=-((\mathbf{S}\cdot(\mathbf{k}\times\mathbf{k}'))^2\frac{1}{q^2}I_2(q)+(\mathbf{k}'\times\mathbf{S})\cdot(\mathbf{k}\times\mathbf{S})\frac{1}{q}I_1(q) \tag{5.17}$$

$\big(\hat{\mathbf{r}}\cdot\boldsymbol{\sigma}_1)(\hat{\mathbf{r}}\cdot\boldsymbol{\sigma}_2) - \frac{1}{3}\boldsymbol{\sigma}_1\cdot\boldsymbol{\sigma}_2\big)$**:**

$$\frac{1}{(2\pi)^3}\int e^{-i\mathbf{k}'\cdot\mathbf{r}}V(r)\left((\hat{\mathbf{r}}\cdot\boldsymbol{\sigma}_1)(\hat{\mathbf{r}}\cdot\boldsymbol{\sigma}_2) - \frac{1}{3}\boldsymbol{\sigma}_1\cdot\boldsymbol{\sigma}_2\right)e^{i\mathbf{k}\cdot\mathbf{r}}d\mathbf{r} =$$
$$-\left((\boldsymbol{\nabla}_q\cdot\boldsymbol{\sigma}_1)(\boldsymbol{\nabla}_q\cdot\boldsymbol{\sigma}_2) - \frac{1}{3}\boldsymbol{\sigma}_1\cdot\boldsymbol{\sigma}_2\boldsymbol{\nabla}_q^2\right)\frac{4\pi}{(2\pi)^3}\int V(r)\frac{r^2}{r^2}j_0(qr)dr =$$
$$-\frac{\boldsymbol{\sigma}_1\cdot\mathbf{q}}{q}\frac{\boldsymbol{\sigma}_2\cdot\mathbf{q}}{q}((I''_{0-}(q) - \frac{I'_{0-}(q)}{q}) - \frac{\mathbf{s}_1\cdot\mathbf{s}_2}{q}I'_0(q) =$$
$$+\frac{1}{3}\boldsymbol{\sigma}_1\cdot\boldsymbol{\sigma}_2(I''_{0-}(q) + \frac{2}{q}I'_{0-}(q)) \tag{5.18}$$

Thus,

$$\frac{1}{(2\pi)^3}\int e^{-i\mathbf{k}'\cdot\mathbf{r}}V(r)\left((\hat{\mathbf{r}}\cdot\boldsymbol{\sigma}_1)(\hat{\mathbf{r}}\cdot\boldsymbol{\sigma}_2) - \frac{1}{3}\boldsymbol{\sigma}_1\cdot\boldsymbol{\sigma}_2\right)e^{i\mathbf{k}\cdot\mathbf{r}}d\mathbf{r} = \left(-\frac{\boldsymbol{\sigma}_1\cdot\mathbf{q}}{q}\frac{\boldsymbol{\sigma}_2\cdot\mathbf{q}}{q} + \frac{\boldsymbol{\sigma}_1\cdot\boldsymbol{\sigma}_2}{3}\right)I_{2-}(q) \tag{5.19}$$

where

$$I_{0-}(q) = \frac{4\pi}{(2\pi)^3}\int V(r)j_2(qr)r^2dr \tag{5.20}$$

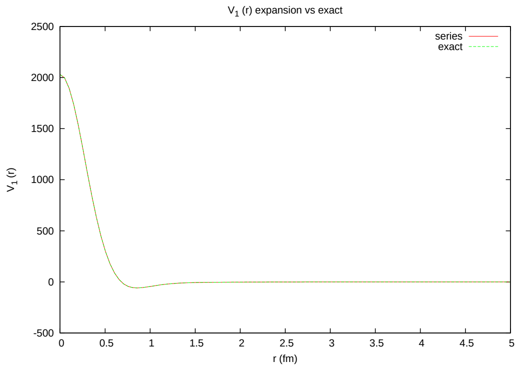

FIG. 1: Calculated $V_1(r)$ compared to exact.

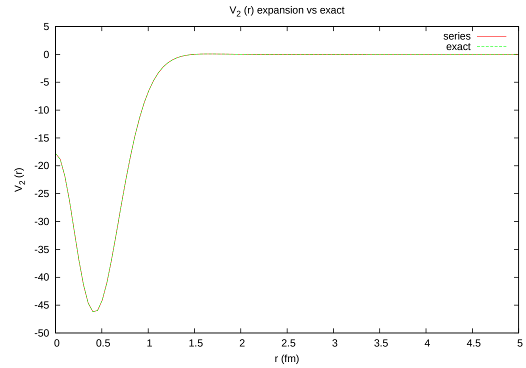

FIG. 2: Calculated $V_2(r)$ compared to exact.

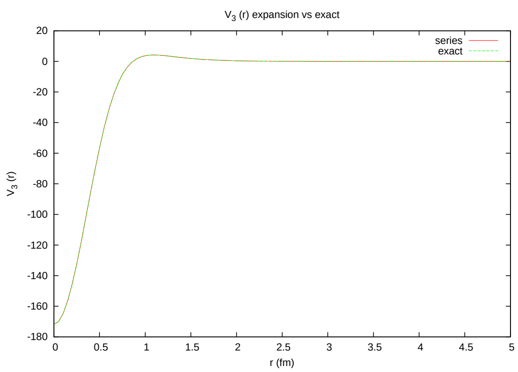

FIG. 3: Calculated $V_3(r)$ compared to exact.

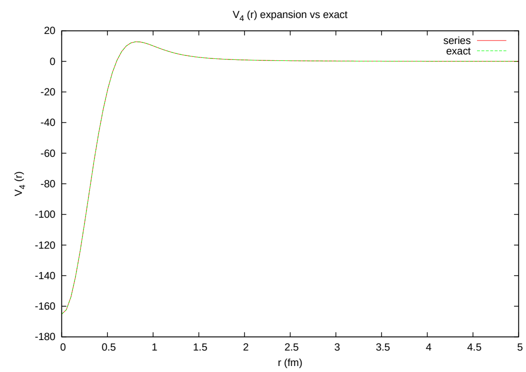

FIG. 4: Calculated $V_4(r)$ compared to exact.

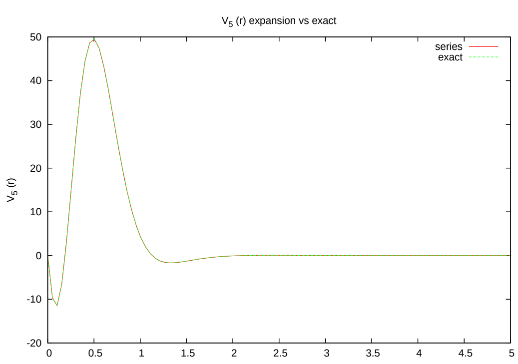

FIG. 5: Calculated $V_5(r)$ compared to exact.

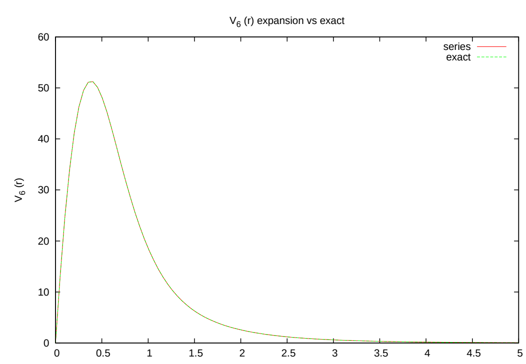

FIG. 6: Calculated $V_6(r)$ compared to exact.

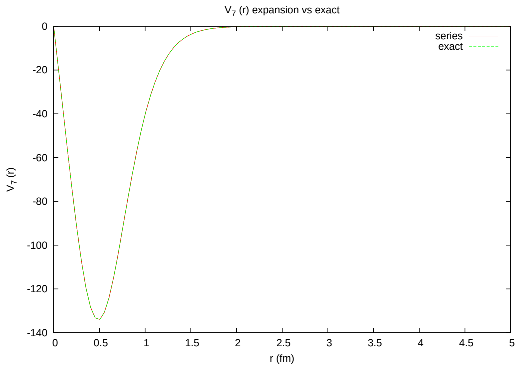

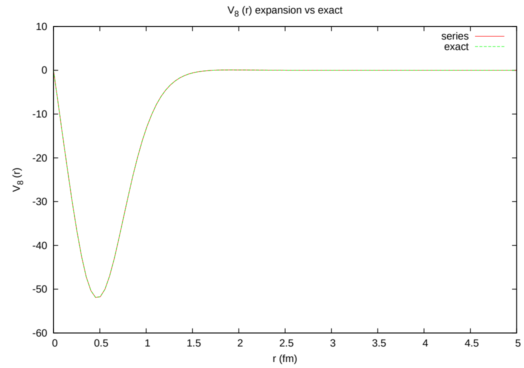

FIG. 7: Calculated $V_7(r)$ compared to exact.

FIG. 8: Calculated $V_8(r)$ compared to exact.

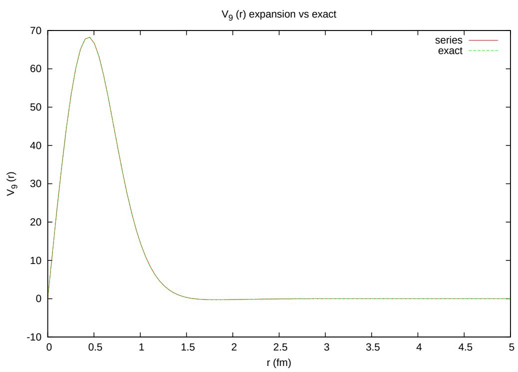

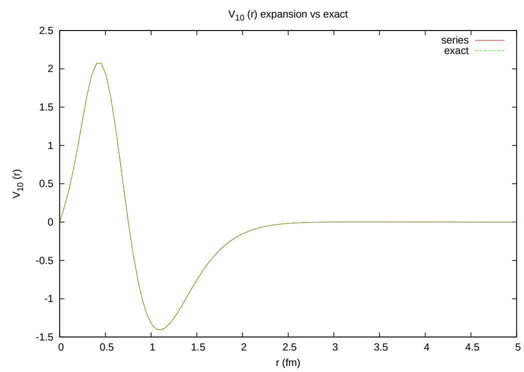

FIG. 9: Calculated $V_9(r)$ compared to exact.

FIG. 10: Calculated $V_{10}(r)$ compared to exact.

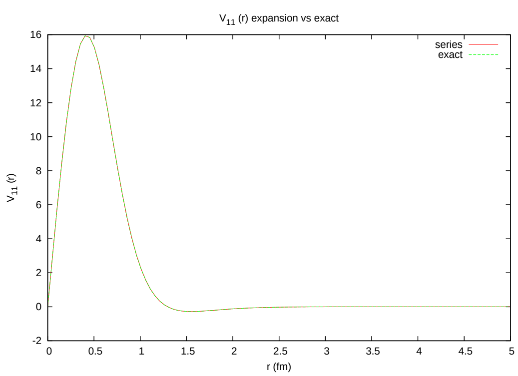

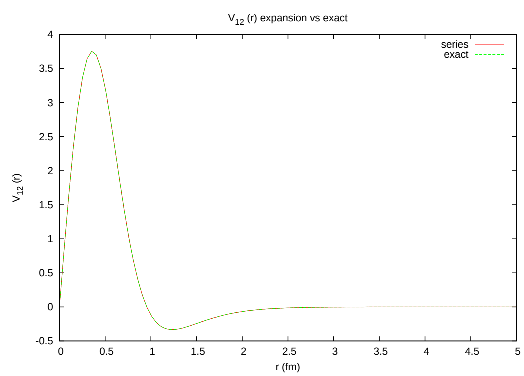

FIG. 11: Calculated $V_{11}(r)$ compared to exact.

FIG. 12: Calculated $V_{12}(r)$ compared to exact.

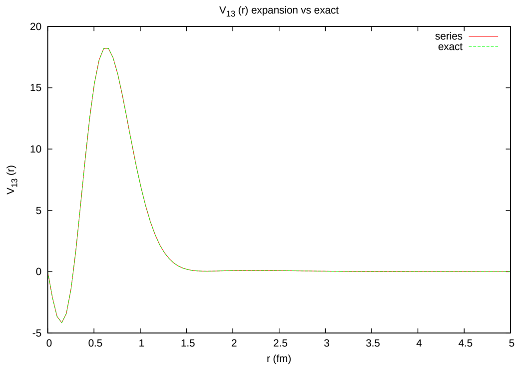

FIG. 13: Calculated $V_{13}(r)$ compared to exact.

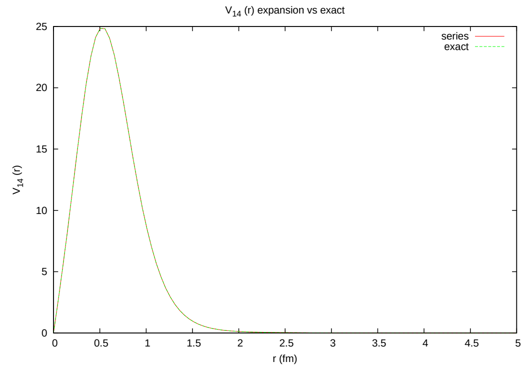

FIG. 14: Calculated $V_{14}(r)$ compared to exact.

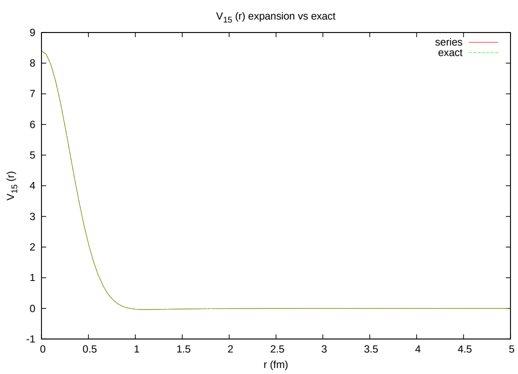

FIG. 15: Calculated $V_{15}(r)$ compared to exact.

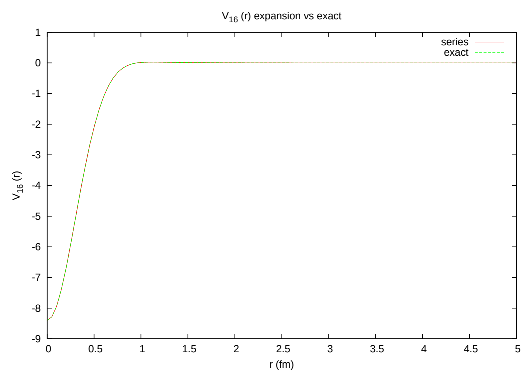

FIG. 16: Calculated $V_{16}(r)$ compared to exact.

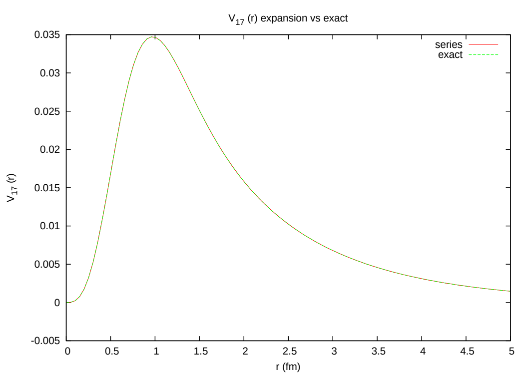

FIG. 17: Calculated $V_{18}(r)$ compared to exact.

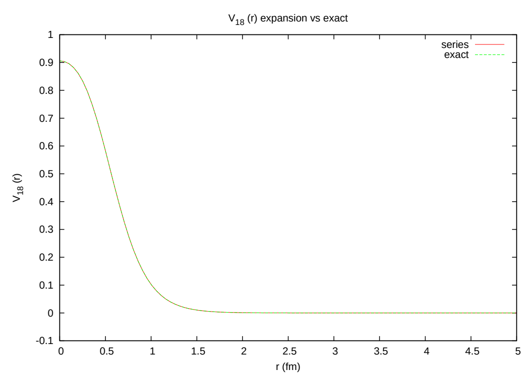

FIG. 18: Calculated $V_{18}(r)$ compared to exact.

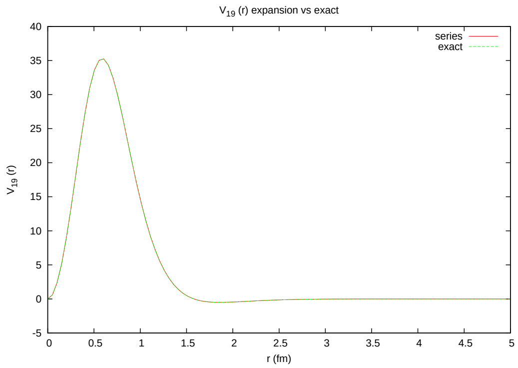

FIG. 19: Calculated $r^2V_9(r)$ compared to exact.

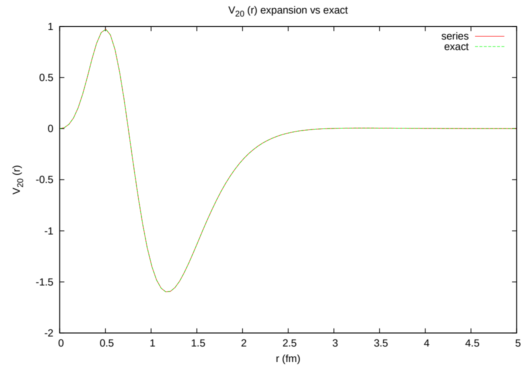

FIG. 20: Calculated $r^2V_{10}(r)$ compared to exact.

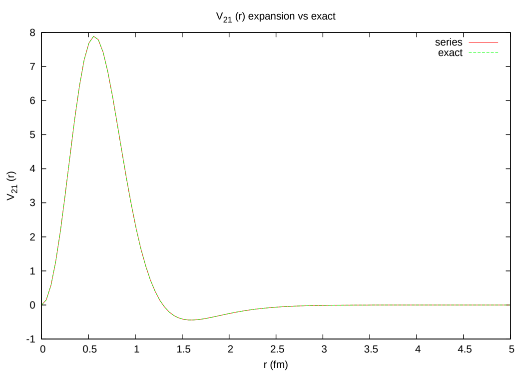

FIG. 21: Calculated $r^2V_{11}(r)$ compared to exact.

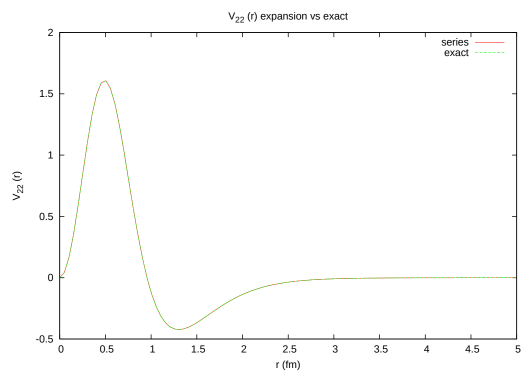

FIG. 22: Calculated $r^2V_{12}(r)$ compared to exact.

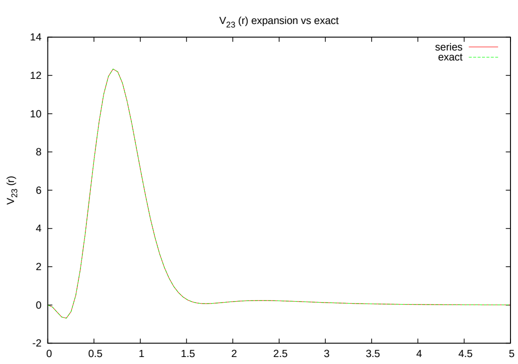

FIG. 23: Calculated $r^2V_{13}(r)$ compared to exact.

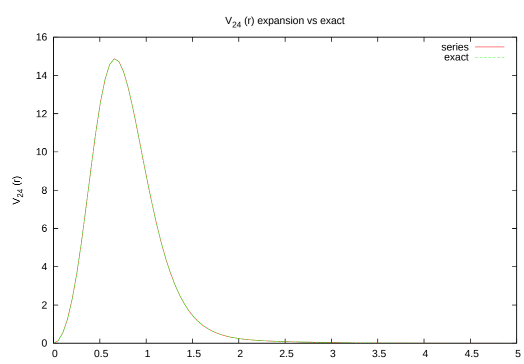

FIG. 24: Calculated $r^2V_{14}(r)$ compared to exact.

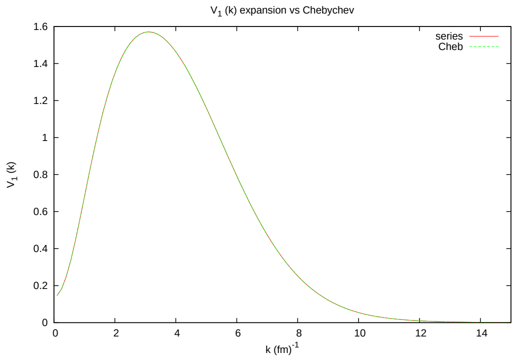

FIG. 25: Calculated $V_1(k)$ compared to Chebyshev.

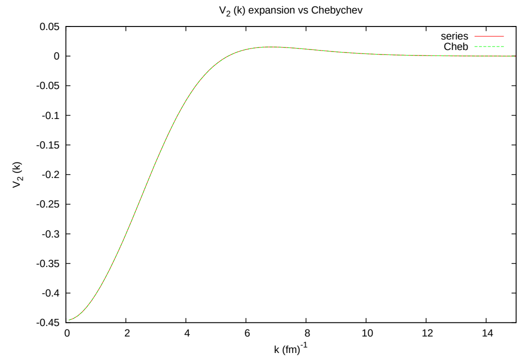

FIG. 26: Calculated $V_2(k)$ compared to Chebyshev.

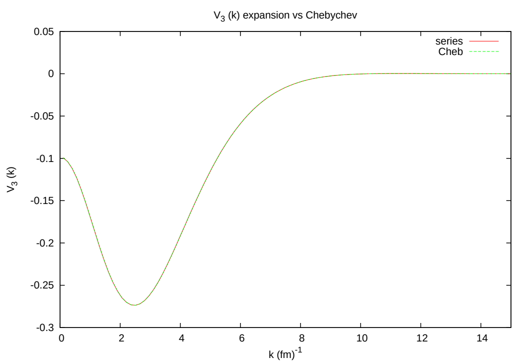

FIG. 27: Calculated $V_3(k)$ compared to Chebyshev.

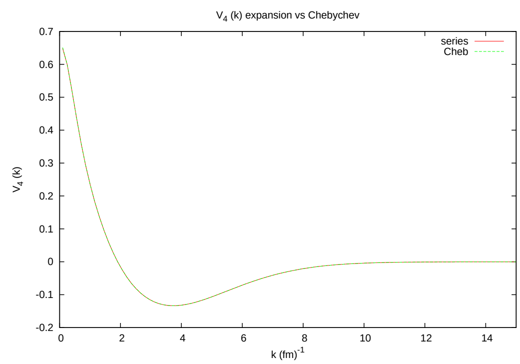

FIG. 28: Calculated $V_4(k)$ compared to Chebyshev.

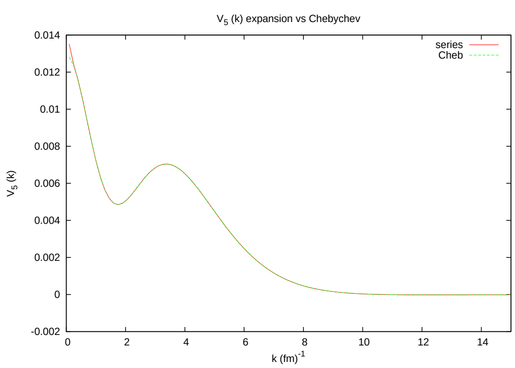

FIG. 29: Calculated $V_5(k)$ compared to Chebyshev.

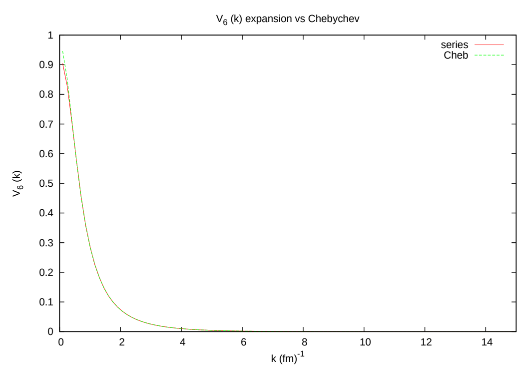

FIG. 30: Calculated $V_6(k)$ compared to Chebyshev.

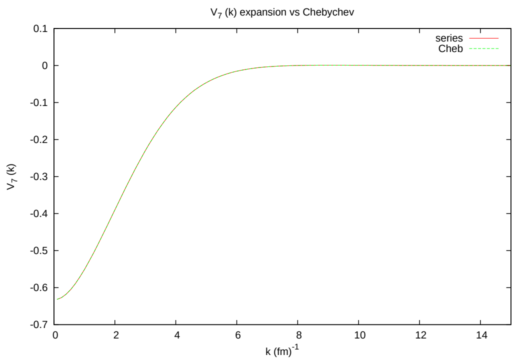

FIG. 31: Calculated $V_7(k)$ compared to Chebyshev.

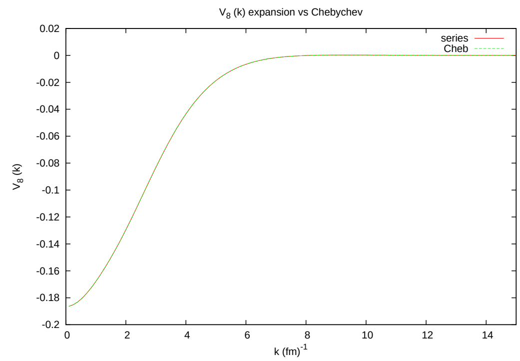

FIG. 32: Calculated $V_8(k)$ compared to Chebyshev.

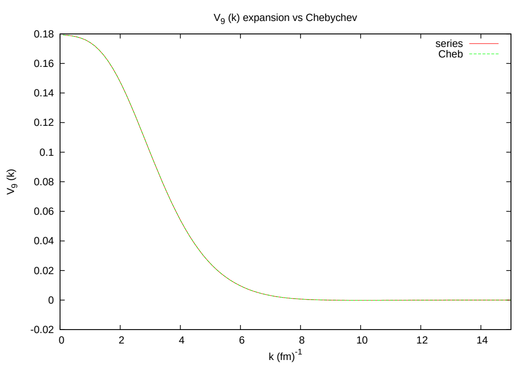

FIG. 33: Calculated $V_9(k)$ compared to Chebyshev.

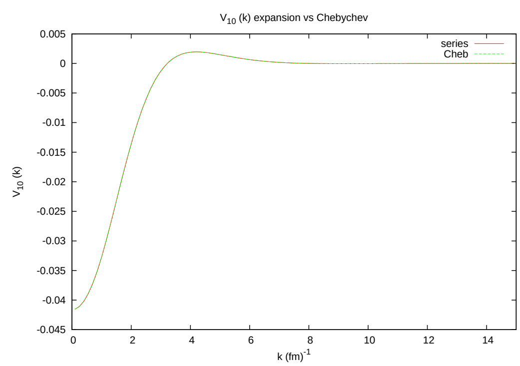

FIG. 34: Calculated $V_{10}(k)$ compared to Chebyshev.

[] R.B. Wiringa, V.G.J. Stoks, R. Schiavilla, Phys. Rev. **C**51(1995) 38.

[] V.G.J. Stoks, R.A.M. Klomp, C.P.F. Terheggen, J. J. de Swart, Phys. Rev. **C**49(1994)2950.

[] R. Machleidt, Phys. Rev. C 63, 024001 (2001)

[] R. Broucke, Communications of the Association for Computing Machinery, 16,(1973)254.

[] B. D. Keister and W. N. Polyzou, J. Comp. Phys. 134, 231(1997).

[] J. Golak, W. Glöckle , R. Skibiński, H. Witała, D. Rozpkedzik, K. Topolnicki, I. Fachruddin, Ch. Elster, A. Nogga, Phys. Rev. C81(2010)034006.

[] Private communication with Robert Wiringa.

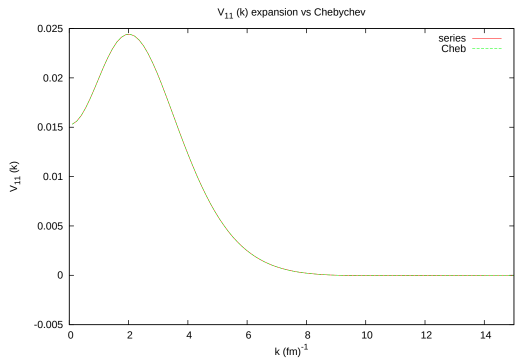

FIG. 35: Calculated $V_{11}(k)$ compared to Chebyshev.

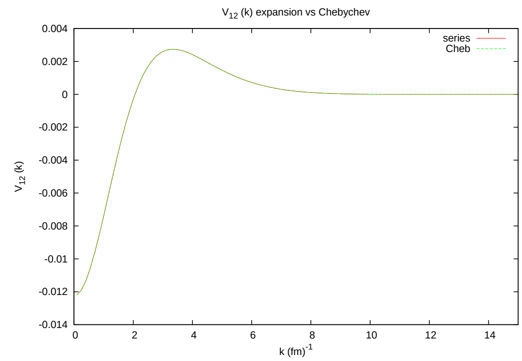

FIG. 36: Calculated $V_{12}(k)$ compared to Chebyshev.

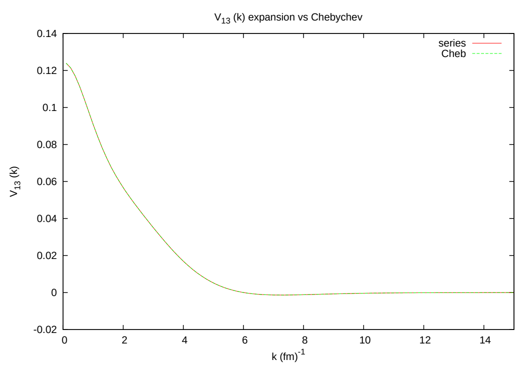

FIG. 37: Calculated $V_{13}(k)$ compared to Chebyshev.

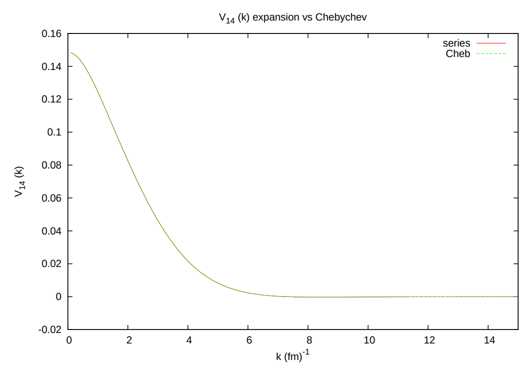

FIG. 38: Calculated $V_{14}(k)$ compared to Chebyshev.

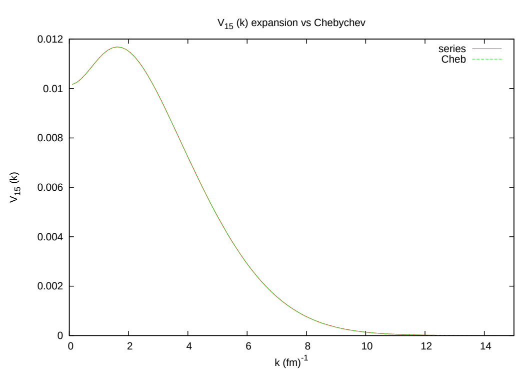

FIG. 39: Calculated $V_{15}(k)$ compared to Chebyshev.

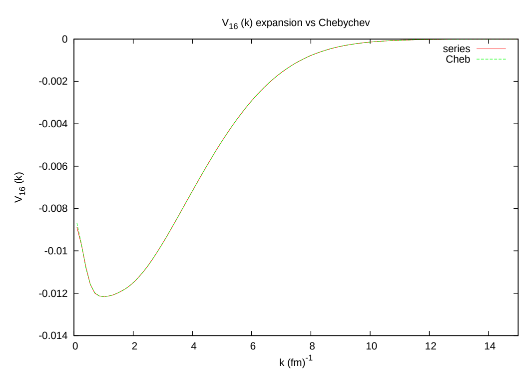

FIG. 40: Calculated $V_{16}(k)$ compared to Chebyshev.

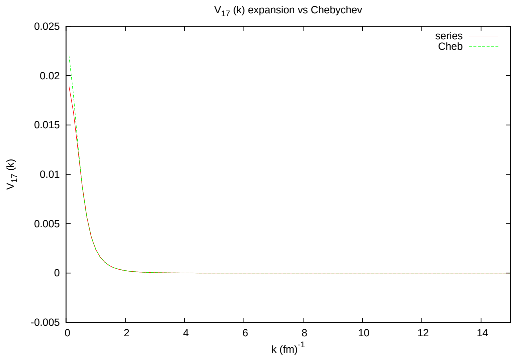

FIG. 41: Calculated $V_{18}(k)$ compared to Chebyshev.

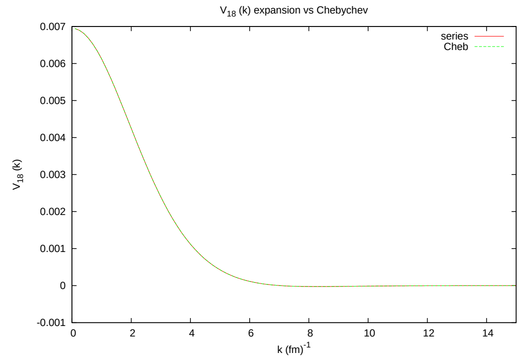

FIG. 42: Calculated $V_{18}(k)$ compared to Chebyshev.

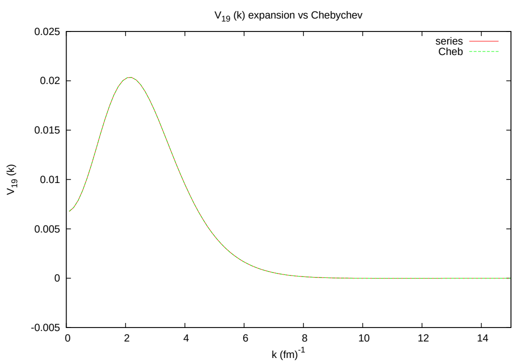

FIG. 43: Calculated $V_{9b}(k)$ compared to Chebyshev.

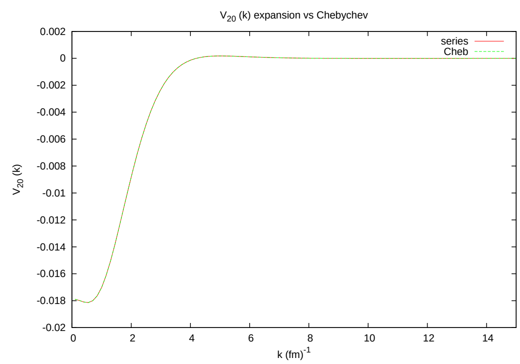

FIG. 44: Calculated $V_{10b}(k)$ compared to Chebyshev.

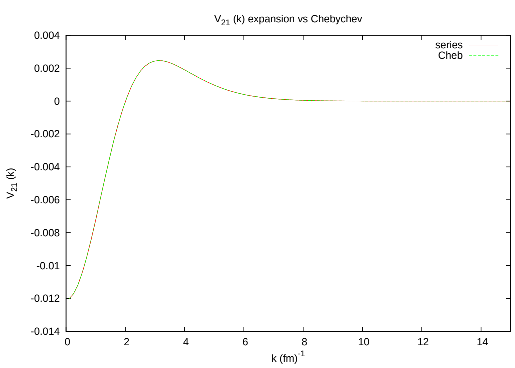

FIG. 45: Calculated $V_{11b}(k)$ compared to Chebyshev.

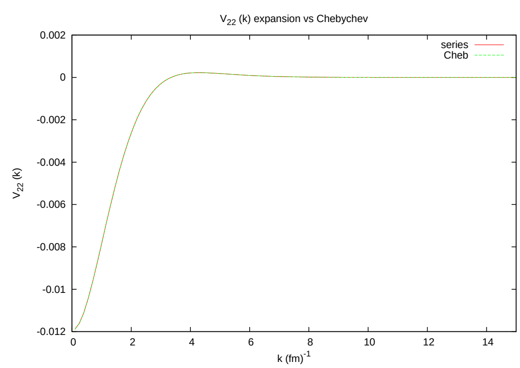

FIG. 46: Calculated $V_{12b}(k)$ compared to Chebyshev.

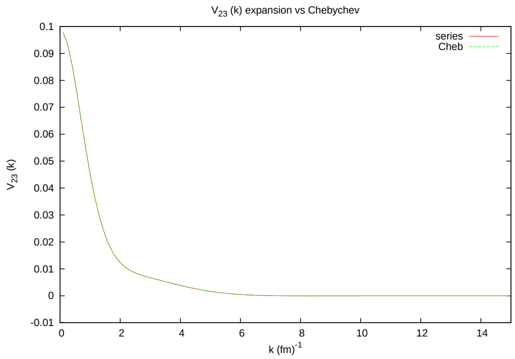

FIG. 47: Calculated $V_{13b}(k)$ compared to Chebyshev.

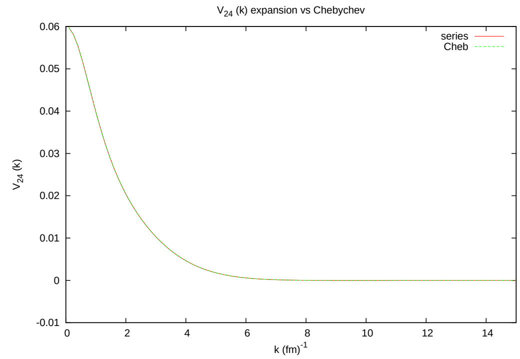

FIG. 48: Calculated $V_{14b}(k)$ compared to Chebyshev.

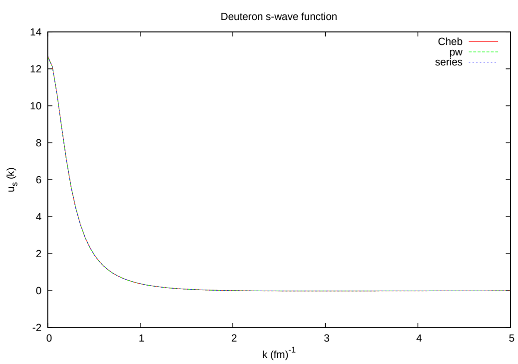

FIG. 49: Deuteron d-state wave function compared to partial wave calculation.

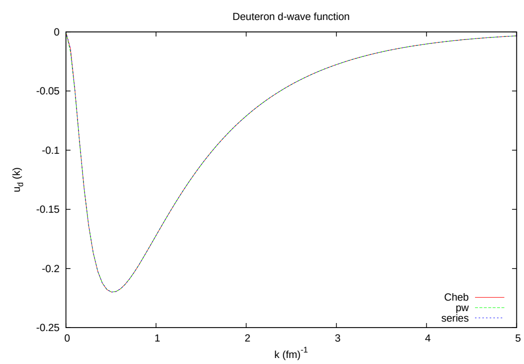

FIG. 50: Deuteron d-state wave function compared to partial wave calculation.